Biochimica et Biophysica Acta 1798 (2010) 1739–1749

Contents lists available at ScienceDirect

Biochimica et Biophysica Acta

journal homepage: www.elsevier.com/locate/bbamem

The plasma membrane plays a central role in cells response to mechanical stress

Sandra V. Verstraeten [a,*], Gerardo G. Mackenzie [b,1], Patricia I. Oteiza [b]

[a] Department of Biological Chemistry, IIMHNO (UBA) and IQUIFIB (UBA-CONICET), School of Pharmacy and Biochemistry, University of Buenos Aires, Junín 956 (C1113AAD), Buenos Aires, Argentina
[b] Departments of Nutrition and Environmental Toxicology, University of California, Davis, One Shields Avenue, Davis, CA 95616, USA

ARTICLE INFO

Article history:
Received 21 January 2010
Received in revised form 7 June 2010
Accepted 9 June 2010
Available online 19 June 2010

Keywords:
Mechanical stress
Membrane fluidity
Calcium
Signal transduction
Lipid lateral mobility

ABSTRACT

The mechanisms by which lymphocytes recognize and interpret mechanical stimuli and translate these into the triggering of select signaling cascades that are critical for lymphocyte function are still not fully understood. In this work, we investigated the association of mechanical stress (MS)-induced changes in membrane physical properties with changes in cytoskeleton dynamics and cell signaling. In Jurkat T cells, MS was associated with the immediate and transient depolymerization of both β-tubulin and F-actin. The fluidity of the plasma membrane measured in the hydrophobic region of the bilayer, increased 0.5 min post-MS, recovering the initial value in the following 2 min. This effect was accompanied by the rearrangement of lipids in the lateral phase of the plasma membrane, transient lipid rafts' alteration, and membrane hyperpolarization. The consequent increase in cellular [Ca^{2+}] triggered the activation of the transcription factors NFAT, AP-1, and NF-κB. Results indicate that the cytoplasmic membrane, through changes in membrane physical properties, senses MS, and transduces an initial physical stimulus into microtubules rearrangements, Ca^{2+} mobilization, and the subsequent changes in cell signaling.

1. Introduction

Tissues are physiologically exposed to mechanical forces that can result in transitory alterations of cell shape by either stretching or compression. This cell deformation can directly or indirectly influence cell functioning, affecting different processes including signal transduction, gene expression, cell growth, differentiation, and survival [1,2]. For example, blood flow over endothelial cells causes a laminar shear stress that stimulates specific integrin/endothelial cells-mediated signaling cascades, leading to cell differentiation [3]. Shear stress also regulates the velocity of endothelial wound closure, with high-pressure stress being associated with a higher rate of cell migration to the wounded area [4]. However, an excessive deformation causes cell damage and, ultimately, cell death, such as that observed in pressure ulcers [5].

Mechanical stress (MS) affects not only attached but also circulating cells, given that they are periodically exposed to a pulsatile blood flow, and establish close interactions with the endothelium during their transit through microvessels. It has been reported that blood flow-mediated cell stress is required to achieve leukocyte transendothelial migration and tissue homing to inflammation sites [6]. MS also causes the reorientation of T lymphocyte pseudopodia, which could be related to a higher endocytotic activity [7]. The effects of MS are not only limited to the stressed cells but can also propagate to surrounding cells. When platelets are submitted to a high shear stress, they activate and produce soluble factors that stimulate the maturation of dendritic cells and T cells' proliferation [8]. Similarly, shear stress causes ATP release from red blood cells, thus participating in blood pressure regulation [9].

Upon MS, several signaling pathways are simultaneously stimulated [1], suggesting the presence of a common upstream mechanoreceptor that transduces the physical deformation of the cell from the surface into its interior yet triggering a biological response. The nature of these mechanoreceptors has not yet been unraveled [10]. We hypothesize that alterations of lipid spatial disposition, clustering,

Abbreviations: 16-AP, 16-(9-anthroyloxy) palmitic acid; 6-AS, 6-(9-anthroyloxy) stearic acid; AP-1, activator protein-1; BODIPY-GM_1, BODIPY® FL C5-ganglioside GM_1; CRAC, Ca^{2+} release-activated Ca^{2+} channels; CsA, cyclosporin A; CTX–FITC, FITC conjugate of subunit B of cholera toxin; $DiBAC_4(3)$, bis-(1,3-dibutylbarbituric acid)trimethine oxonol; DTT, dithiothreitol; FBS, fetal bovine serum; HRP, horseradish peroxidase; IKKβ, inhibitor of nuclear factor kappa B kinase beta subunit; IκBα, I-kappa-B kinase alpha; JNK, Jun N-terminal kinase; MAPK, mitogen-activated protein kinase; MAPKK, kinase of mitogen-activated protein kinase; MS, mechanical stress; NFAT, nuclear factor of activated T cells; NF-kB, nuclear factor kappa B; PKC, protein kinase C; PLCγ, phospholipase C gamma; p-NFAT, phosphorylated nuclear factor of activated T cells; TNFα, tumor necrosis factor alpha

* Corresponding author. Departamento de Química Biológica, IQUIFIB (UBA-CONICET), Facultad de Farmacia y Bioquímica, Universidad de Buenos Aires. Junín 956 (C1113AAD), Buenos Aires, Argentina. Tel.: +54 11 4964 8287; fax: +54 11 4962 5457.
E-mail address: verstraeten@ffyb.uba.ar (S.V. Verstraeten).
[1] Permanent address: Division of Cancer Prevention, Department of Medicine, Stony Brook University, Stony Brook, NY 11794-5200, USA.

0005-2736/$ – see front matter © 2010 Elsevier B.V. All rights reserved.
doi:10.1016/j.bbamem.2010.06.010

freedom of mobility, and/or their interactions with membrane proteins could be the link between MS and signal transduction. If true, changes in membrane fluidity and lipid distribution could result in alterations in the distribution and/or composition of lipid rafts, and of cytoskeleton assembly, being both scaffolds for signaling molecules. In this work, we present evidence that MS causes a transient increase in plasma membrane fluidity that is associated with both β-tubulin and F-actin disassembly and changes in the arrangement of lipid rafts in the membrane. MS is also associated with an increase in cytosolic Ca^{2+} content as a result of both influx and intracellular mobilizations. This rise in cellular Ca^{2+} content triggers the activation of transcription factors NFAT, NF-κB, and AP-1 known to be involved in T-cell activation.

2. Material and methods

2.1. Chemicals

The fluorescent probes 6-(9-anthroyloxy)stearic acid (6-AS), 16-(9-anthroyloxy) palmitic acid (16-AP), FURA 2-AM, bis-(1,3-dibutylbarbituric acid)trimethine oxonol ($DiBAC_4(3)$), pyrene, BODIPY® FL C5-ganglioside GM_1 (BODIPY-GM_1), subunit B of cholera toxin conjugated with FITC (CTX–FITC), and BODIPY® TR-X phallacidin were purchased from Invitrogen/Molecular Probes Inc. (Eugene, OR, USA). The inhibitors U73122, TMB-8, BAPTA-AM, Ro 32-0432, cyclosporin A (CsA), and SKF96365 were obtained from Calbiochem (La Jolla, CA, USA). RPMI 1640 medium, streptomycin, penicillin, and fetal bovine serum (FBS) were purchased from Gibco BRL (Grand Island, NY, USA). The oligonucleotide containing the consensus sequence for NF-κB, AP-1, and OCT-1 and the reagents for the EMSA assay were obtained from Promega (Madison, WI, USA). The protease inhibitor cocktail was obtained from Roche Applied Science (Mannheim, Germany). The oligonucleotide containing the consensus sequence for NFAT, and antibodies for p-p38, p-JNK2, JNK, NFATc3, and IκBα were obtained from Santa Cruz Biotechnology (Santa Cruz, CA, USA). PVDF membranes were obtained from Bio-Rad (Hercules, CA, USA), and Chroma Spin-10 columns were from Clontech (Palo Alto, CA, USA). The ECL Western blotting system was obtained from GE Healthcare (Piscataway, NJ, USA). Bis-benzimide H (Hoechst 32258) and all other reagents were from the highest quality available and were purchased from Sigma (St. Louis, MO, USA).

2.2. Cell culture and mechanical stress (MS)

Human leukemia T cells (Jurkat) were obtained from the American Type Culture Collection (ATCC, Rockville, MD, USA). Jurkat T cells were cultured at 37 °C in a 5% CO_2 atmosphere, in RPMI 1640 medium, supplemented with 2 mM L-glutamine, 10% (vol./vol.) FBS, and penicillin (50 U/ml) and streptomycin (50 μg/ml).

Twenty-four hours before the experiments, cells were centrifuged for 10 min at $800\times g$; the number of viable cells was determined by the Trypan Blue dye-exclusion method and suspended in culture medium to a density of 1×10^6 cells/ml. For the experiments, mechanical stress (MS) was imposed to the cell suspension by a 5-times passage through a 200-μm-diameter, 23-mm-length plastic tube connected to a plastic syringe, and with a flow of 0.35 ± 0.05 ml/s. Since Jurkat T cells do not spontaneously adhere to plastic, no cell–matrix interactions are expected. On the other hand, at the cell concentration used for the experiments (1×10^6 cells/ml), the overall cellular volume represented only 0.059% of total cell suspension volume, thus minimizing cell–cell interactions during MS. Therefore, the main forces participating in this MS model might be a pressure gradient between both ends of the tube and the turbulence generated both during their transit through the tube and at the end of it. We evaluated whether this approach affected cell viability, with no decrease in the number of viable cells observed after this procedure.

2.3. Evaluation of F-actin content

At 1–60 min after MS, cells were fixed by incubating for 20 min at room temperature with an equal volume of ice-cold 4% (wt./vol.) paraformaldehyde. Cells were centrifuged for 10 min at $800\times g$, the supernatant was discarded, and the cell pellet was washed twice with phosphate-buffered saline (PBS). After a 5-min incubation in the presence of 0.1% (vol./vol.) Triton X-100 in PBS, cells were washed twice with PBS and incubated for 30 min at room temperature in the presence of 10 U of BODIPY TR-X phallacidin [11]. The fluorescence of the complex F-actin-BODIPY TR-X phallacidin was measured at 617 nm ($\lambda_{excitation}=560$ nm) in a Kontron SFM-25 spectrofluorometer (Kontron Instruments sPA, Milan, Italy) equipped with temperature control and a 10-nm monochromator bandwidth. Results were corrected by the DNA content in the samples evaluated by reacting with 25 μM Hoechst 32258 ($\lambda_{excitation}=346$ nm, $\lambda_{emission}=460$ nm).

2.4. Soluble/polymerized β-tubulin distribution

After MS, polymerized, soluble, and total β-tubulin extracts were prepared basically as previously described [12]. To isolate the soluble and polymeric microtubule fractions, cells (3×10^6) were washed gently in a microtubule stabilization buffer (MTSB) containing 0.1 M PIPES, pH 6.75, 1 mM EGTA, 1 mM $MgSO_4$, 2 M glycerol, and Mini EDTA-free protease inhibitor cocktail. Cells were incubated at 37 °C for 10 min with 0.5 ml of MTSB containing 0.1% (vol./vol.) Triton X-100. The supernatant (soluble tubulin fraction) was removed and centrifuged at $800\times g$ for 10 min. The remaining Triton-extracted cytoskeletal ghosts were subsequently solubilized by adding 0.5 ml of lysis buffer (25 mM Tris–HCl, pH 7.4, 0.4 M NaCl, and 0.5% (wt./vol.) SDS) constituting the polymerized tubulin fraction. Total tubulin was extracted by addition of lysis buffer directly to intact cells cultured in six-well plates. All extraction steps were performed at 37 °C. Soluble, polymerized, and total β-tubulin fractions were analyzed by Western blot as described below.

2.5. Evaluation of membrane fluidity

Jurkat cells were labeled with either the fluorescent probe 6-AS or 16-AP (probe–lipid ratio ~ 1:500). Cells were incubated at 37 °C for 15 min to allow the incorporation of the probe to the plasma membrane. A 200-μl aliquot of cell suspension was separated to measure baseline plasma membrane fluidity, and the remaining cells were submitted to MS as described above. Membrane fluidity was evaluated at 37 °C from the fluorescence polarization (P) of the probes using the following equation:

$$P=\frac{\left(I_{//}-I_{\perp}\right)}{\left(I_{//}+I_{\perp}\right)}$$

where $I_{//}$ and $I_{\perp}$ are the fluorescence intensities at 435 nm ($\lambda_{excitation}=384$ nm) with the emission polarizer oriented parallel or perpendicular to the excitation polarizer, respectively.

2.6. Evaluation of plasma membrane lipid lateral mobility

The probe pyrene, a fluorescent molecule that evenly distributes in the bilayer, was used to evaluate lipid lateral mobility. An increase in lipid mobility facilitates the collision of two molecules of pyrene forming an excited state (excimer) [13]. Jurkat cells were incubated at 37 °C for 15 min in the presence of pyrene (probe:lipid ratio ~ 1:500) to allow the incorporation of the probe to the cytoplasmic membrane. A 200-μl aliquot of cell suspension was separated to measure baseline fluorescence, and the remaining cells were submitted to MS as described above. Membrane lateral phase

separation was evaluated at 37 °C as the ratio between pyrene excimer ($\lambda_{emission} = 465$ nm) and monomer ($\lambda_{emission} = 390$ nm) fluorescence emission ($\lambda_{excitation} = 340$ nm).

2.7. Evaluation of lipid rafts' integrity

Lipid rafts' integrity was evaluated using two different fluorescent probes. First, Jurkat T cells were incubated for 15 min at 37 °C in the presence of 0.17 μM BODIPY-GM_1. In the second situation, Jurkat T cells were incubated for 30 min at 4 °C in the presence of 10 μg/μl of the subunit B of cholera toxin conjugated with FITC (CTX–FITC). Samples were centrifuged for 5 min at 800×*g* to eliminate the excess of probe. Pellets were then washed twice with warm PBS and suspended in PBS. Cells labeled with either BODIPY-GM_1 or CTX–FITC were submitted to MS as described above and were further incubated for 1, 15, or 30 min at 37 °C. At the different time points, 20-μl aliquots were taken, and samples were analyzed by epifluorescence using an Olympus BX50 microscope (Tokyo, Japan). The distribution of the fluorescence was analyzed using an Image Pro Plus v.5.1 software (Media Cybernetics, Sylver Spring, MD, USA).

2.8. Evaluation of plasma membrane potential

Jurkat T cells were incubated for 15 min at 37 °C in the presence of 1.5 μM $DiBacC_4(3)$. A 200-μl aliquot of cell suspension was separated, centrifuged for 5 min at 800×*g*, suspended in PBS, and used to register the baseline value. The remaining cells were submitted to MS as described above, separated into 200-μl aliquots, and incubated at 37 °C for 1 to 40 min. After incubation, cells were centrifuged as above, suspended in PBS, and the fluorescence was measured at 515 nm ($\lambda_{excitation} = 490$ nm). Results were normalized by DNA content in the samples using Hoechst 32258, as described above.

2.9. Evaluation of intracellular Ca^{2+} content

Changes in the intracellular content of Ca^{2+} were evaluated from the fluorescence of the probe FURA 2-AM [14]. Jurkat T cells were incubated for 30 min at 37 °C in the presence of 5 μM FURA 2-AM. After incubation, cells were centrifuged for 5 min at 800×*g* and suspended in PBS. A 200-μl aliquot of cell suspension was separated to measure baseline Ca^{2+} content, and the remaining cells were submitted to MS as described above. Ca^{2+} content was estimated from the emission at 510 nm ($\lambda_{excitation} = 340$ and 380 nm). Maximal and minimal FURA binding to Ca^{2+} were measured after cell disruption with Igepal (0.01% vol./vol.) in the presence of either 5 mM Ca^{2+} or 25 mM EGTA, respectively.

2.10. Electrophoretic mobility shift assay (EMSA)

Total and nuclear cell fractions were prepared as previously described [15]. Protein concentration was determined by the method of Bradford [16], and samples were stored at −80 °C until use. For the EMSA, the oligonucleotides containing the consensus sequences for NFAT, NF-κB, AP-1, or OCT-1 were end-labeled with [γ-^{32}P] ATP using T4 polynucleotide kinase and purified using Chroma Spin-10 columns. Samples were incubated with the labeled oligonucleotide (20,000–30,000 cpm) for 20 min at room temperature in 10 mM Tris–HCl buffer, pH 7.5, containing 4% (vol./vol.) glycerol, 1 mM $MgCl_2$, 0.5 mM EDTA, 0.5 mM DTT, 50 mM NaCl, and 0.05 mg/ml poly(dI-dC). The products were separated by electrophoresis in a 4% (wt./vol.) nondenaturing polyacrylamide gel using 0.5×TBE (45 mM Tris/borate, 1 mM EDTA) as the running buffer. The gels were dried, and radioactivity was quantitated in a Phosphoimager 840 (GE Healthcare, Piscataway, NJ, USA).

2.11. Western blot analysis

To evaluate the phosphorylation of IκBα, p38, and JNK, cell lysates were prepared in SDS sample buffer (62.5 mM Tris–HCl buffer, pH 6.8, containing 2% (wt./vol.) SDS, 10% (vol./vol.) glycerol, 50 mM DTT, and 0.01% (wt./vol.) bromophenol blue), sonicated for 15 s to shear DNA and reduce sample viscosity, and then heated at 95 °C for 5 min. Immediately, 30 μl of the lysate was loaded onto SDS–PAGE. Proteins were separated by reducing 10%–12.5% (wt./vol.) polyacrylamide gel electrophoresis and electroblotted to PVDF membranes. Colored molecular weight standards (GE Healthcare, Piscataway, NJ, USA) were ran simultaneously. Membranes were blocked overnight in 5% (wt./vol.) nonfat milk and incubated in the presence of the corresponding primary antibodies (1:1000 dilution) for 90 min at 37 °C. After incubation for 90 min at room temperature in the presence of the secondary antibody (HRP-conjugated) (1:10,000 dilution), the conjugates were visualized by reacting with chemiluminescent ECL Western blotting detection reagent in a Phosphoimager 840. The membranes were normalized by reblotting with the antibody for the corresponding nonphosphorylated form of each protein.

2.12. Statistics

One-way analysis of variance (ANOVA) followed by Fisher's PLSD (protected least square difference) test was performed using the routines available in StatView 5.0 (SAS Institute, Cary, NC, USA). Two-way ANOVA was performed using the software GraphPad Prism 4.0 for Windows (GraphPad Software, San Diego, CA, USA). A probability (P) value lower than 0.05 was considered statistically significant.

3. Results

3.1. MS causes the disassembly of actin and tubulin networks

To evaluate whether MS could modify cytoskeleton organization, actin and tubulin polymerization was evaluated. The dynamics of the actin network was evaluated for 1–60 min after MS by reacting with the fluorescent probe BODIPY TR-X phallacidin that specifically binds to F-actin. As shown in Fig. 1A, the content of F-actin decreased immediately after MS, reaching a minimum of 5 min after MS (50% decrease respect to nonstressed cells, $P<0.001$), and progressively recovering the initial value at longer periods of incubation.

To assess the extent of tubulin assembly, polymerized and soluble tubulin fractions were isolated from control and MS cells and analyzed by Western blot. At 1 min after MS, a 43% decrease in the content of polymerized tubulin was found compared to nonstressed cells ($P<0.001$) (Fig. 1B). This ratio progressively increased at longer incubation times, reaching a maximum around 30 min after MS ($P<0.005$), and returning to baseline values at 60 min after MS (Fig. 1B).

3.2. MS promotes alterations in plasma membrane physical properties

The potential effects of MS on Jurkat T cells plasma membrane fluidity were next investigated. Before MS, cells were labeled with the fluorescent probes 6-AS or 16-AP. These probes sense the fluidity of their environment at different depths of the bilayer, with 6-AS being located at the level of the glycerol backbone of phospholipids (~7 Å), while 16-AP resides in the hydrophobic core of the membrane (~16 Å) [17]. With 6-AS, no changes in membrane fluidity were observed in cells under MS compared to control cells in all the tested period (data not shown). In 16-AP-labeled cells, a significant decrease in fluorescence polarization was observed immediately after MS ($P<0.005$; Fig. 2A), indicating an increase in membrane fluidity. Two minutes after MS, plasma membrane fluidity returned to basal values

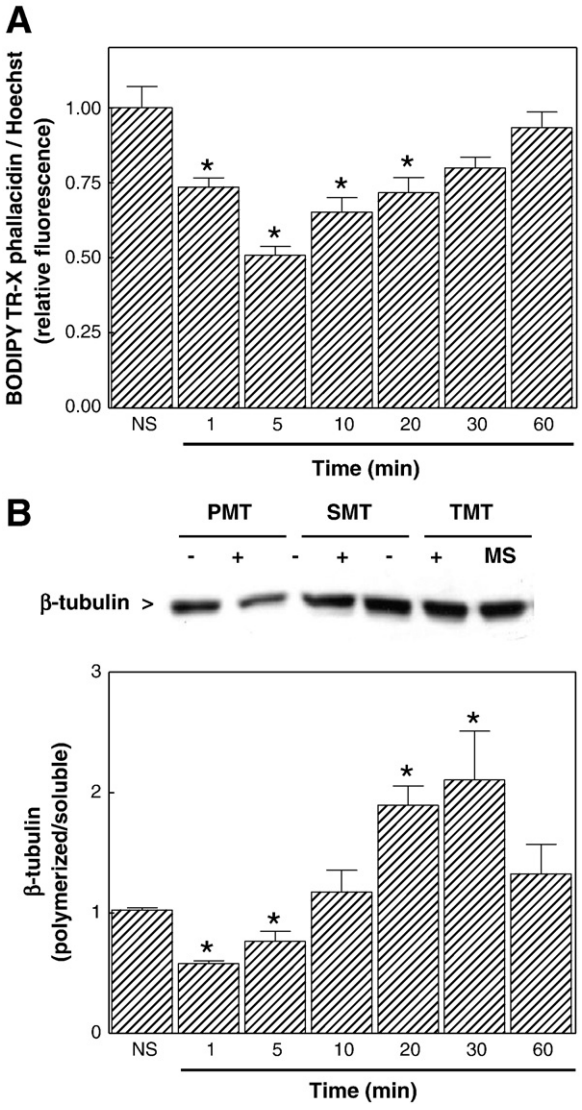

Fig. 1. MS causes F-actin and β-tubulin disassembly. (A) F-actin content was measured 1–60 min after MS by reacting with BODIPY TR-X phallacidin, as described in Material and methods. Results are shown as the mean ± SEM of four independent experiments. *Significantly different to the value measured in nonstressed (NS) cells ($P<0.005$). (B) The content of polymerized (PMT), soluble (SMT), and total (TMT) tubulin was evaluated by Western blot analysis before or after (1–60 min) submitting Jurkat T cells to MS. Top panel: a representative Western blot showing relative tubulin content in cells before (−) or 1 min after MS (+). Bottom panel: kinetics of changes in the ratio polymerized/soluble tubulin in nonstressed (NS) and 1–60 min after MS. Results are shown as the mean ± SEM of four independent experiments. *Significantly different to the value measured in nonstressed cells ($P<0.01$).

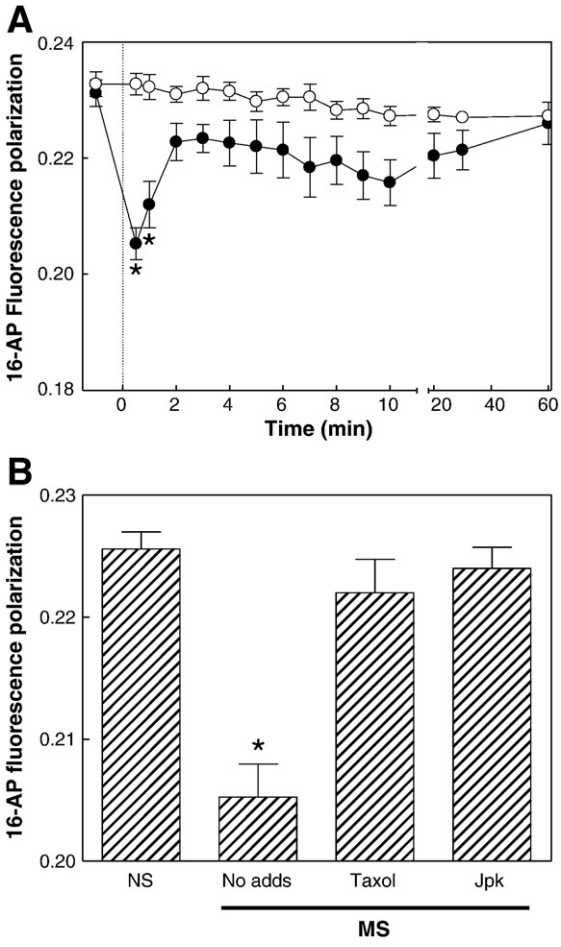

Fig. 2. MS affects plasma membrane fluidity in the hydrophobic region of the bilayer. Plasma membrane fluidity was evaluated in Jurkat T cells from the changes in the fluorescence polarization of the probe 16-AP, as indicated in Material and methods. (A) Kinetics of changes in 16-AP fluorescence polarization in nonstressed (○) and in MS cells (●). Dotted line indicates the moment where MS was performed. (B) 16-AP fluorescence polarization was measured in nonstressed (NS) cells, in cells submitted to MS (no adds), and in cells preincubated for 1 h at 37 °C with 1 μM Taxol (Taxol) or 100 nM jasplakinolide (Jpk) and subsequently submitted to MS. Fluorescence polarization was measured 1 min after MS. Results are shown as the mean ± SEM of four independent experiments. *Significantly different to the value measured in nonstressed cells ($P<0.01$).

(Fig. 2A). When cells were incubated for 3 h before the MS in the presence of compounds that stabilize microtubules (taxol) and microfilaments (jasplakinolide), the decrease of 16-AP fluorescence polarization by MS was prevented (Fig. 2B). These findings stress the relevance of the cytoskeleton in the regulation of cell membrane fluidity during MS.

To evaluate whether these changes in plasma membrane fluidity were associated with a lateral rearrangement of lipids in the bilayer, cells were labeled with the fluorescent probe pyrene. In nonstressed cells, no changes in pyrene excimer to monomer fluorescence ratio (E/M) were observed through all the tested period. On the contrary, in cells submitted to MS, a time-dependent decrease in E/M ratio was observed compared to nonstressed cells (Fig. 3). This effect was significant ($P<0.005$) even after 1 min after MS and reached a plateau after 15 min after MS. The possibility that the lateral arrangement of

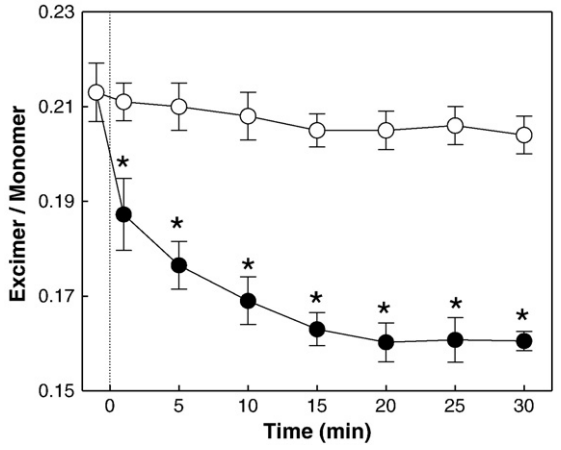

Fig. 3. MS causes lipid rearrangement in the lateral phase of the cell plasma membrane. Jurkat T cells labeled with the fluorescent probe pyrene were submitted (●) or not (○) to MS as indicated in Material and methods. Lipid lateral phase separation was evaluated from the pyrene excimer-to-monomer (E/M) fluorescence ratio. Results are shown as the mean ± SEM of five independent experiments. *Significantly different ($P<0.005$) from the value measured in nonstressed cells. Dotted line indicates the moment where MS was performed.

lipids after MS could be associated with the disassembly of membrane lipid rafts was next investigated. For this purpose, the distribution of a fluorescent derivative of GM_1 (BODIPY-GM_1), which is proposed to label lipid rafts, was evaluated by fluorescence microscopy. Before MS, cell plasma membrane labeling was polarized, showing small patches with no labeling (Fig. 4, left panels). This polarization in membrane location of the probe was enhanced by MS, suggesting a probe's clustering, being the initial pattern of labeling recovered after 30 min after MS. In a separate set of experiments, the endogenous pool of ganglioside GM_1 in plasma membrane was labeled with CTX–FITC, a probe widely used to monitor lipid rafts' dynamics [18,19]. This approach was selected to minimize the possible side effects of the incorporation of a labeled lipid into plasma membrane. In resting cells, plasma membrane labeling showed a homogenous distribution (Fig. 4, right panels). Upon MS, fluorescence concentrated into discrete spots, recovering the initial pattern of distribution after 30 min of incubation. Together, these findings suggest that, following MS, certain membrane domains (most likely lipid rafts) are altered, which could lead to the triggering of associated signaling pathways.

The possibility that MS could cause changes in cell plasma membrane polarization was next studied. Cells were loaded with

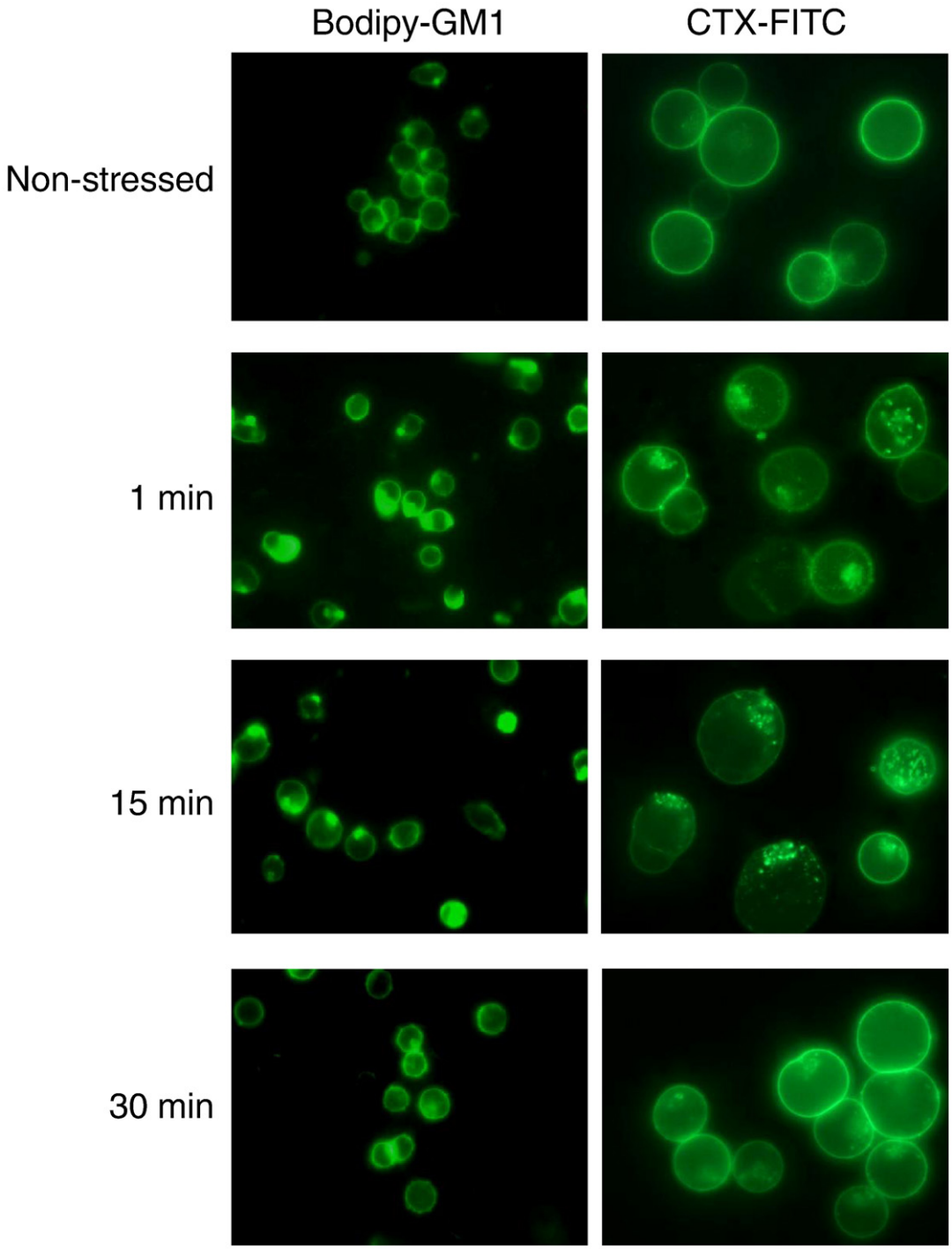

Fig. 4. MS alters lipid rafts' distribution in the cell plasma membrane. Jurkat T cells were either labeled with the fluorescent probe BODIPY-GM_1 (left panels), or with CTX–FITC (right panels). The distribution of the probes in the plasma membrane was evaluated by fluorescence microscopy in nonstressed cells, or after 1, 15, or 30 min after MS. Magnification: 600× (BODIPY-GM_1) and 1000× (CTX–FITC).

the fluorescent probe DiBacC_4(3), a water-soluble, voltage-sensitive molecule that freely crosses the plasma membrane according to its potential [20]. The higher the transmembrane potential, the lower the internalization of the probe. In nonstressed cells, the fluorescence of the probe within cells was similar throughout the studied period (60 min) (Fig. 5). A significant decrease in DiBacC_4(3) fluorescence occurred as a consequence of MS (Fig. 5). This effect was observed 1 min after MS and fluorescence remained low throughout the 60-min incubation period. These results suggest that MS induces cell hyperpolarization, an effect that could be related to changes in ion fluxes, such as Ca^{2+}.

3.3. MS leads to Ca^{2+} mobilization

Intracellular Ca^{2+} content was next investigated measuring the changes in Fura 2-AM fluorescence. In Jurkat T cells incubated in a Ca^{2+}-free medium, and submitted to MS, a significant increase (~150 nM) in Ca^{2+} content was observed 1 min after MS compared to nonstressed cells ($P<0.001$). This effect was sustained up to 30 min after MS (Fig. 6A). When cells were incubated in cell culture medium containing 1 mM Ca^{2+}, the cellular concentration of Ca^{2+} was higher (Fig. 6B) in MS cells compared to nonstressed cells. Fluorescence increased continuously along the incubation period (0–60 min).

To characterize the source of Ca^{2+} after MS, cells were preincubated with different inhibitors of Ca^{2+} mobilization. Thus, cells were preincubated in the presence of inhibitors of PLCγ (U73122), Ca^{2+} release from the endoplasmic reticulum (TMB-8), or store-operated Ca^{2+} channels (SKF96365). For all the inhibitors used, Ca^{2+} content remained within control values upon MS (Fig. 6B).

3.4. MS leads to the activation of NFAT, NF-κB, and AP-1 signaling cascades

We next studied the effects of MS on the activation of transcription factors NFAT, NF-κB and AP-1. To investigate the total levels of activation, DNA binding of the different transcription factors were measured in total cell extracts by EMSA, and the upstream NF-κB (IκBα phosphorylation) and AP-1 (p38 and JNK phosphorylation) were measured by Western blot.

The maximum NFAT–DNA binding was observed 20 min after MS (Figs. 7B and E). An increase in AP-1–DNA binding was also observed, reaching a maximum value 30 min after MS (Figs. 7C and E). The

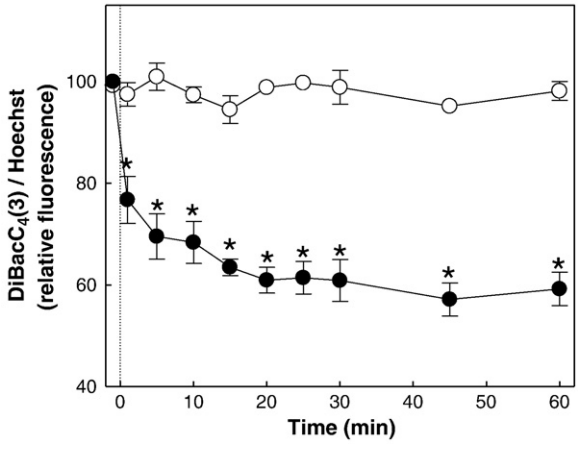

Fig. 5. MS causes plasma membrane hyperpolarization. Jurkat T cells were loaded with the fluorescent probe DiBacC_4(3) as described in Material and methods, and submitted (●) or not (○) to MS. At the different time points after MS cell fluorescence was registered, and normalized by the DNA content in the samples using the probe Hoechst 32258. Results are shown as the mean ± SEM of four independent experiments. *Significantly different from the value measured in nonstressed cells ($P<0.001$, two-way ANOVA test).

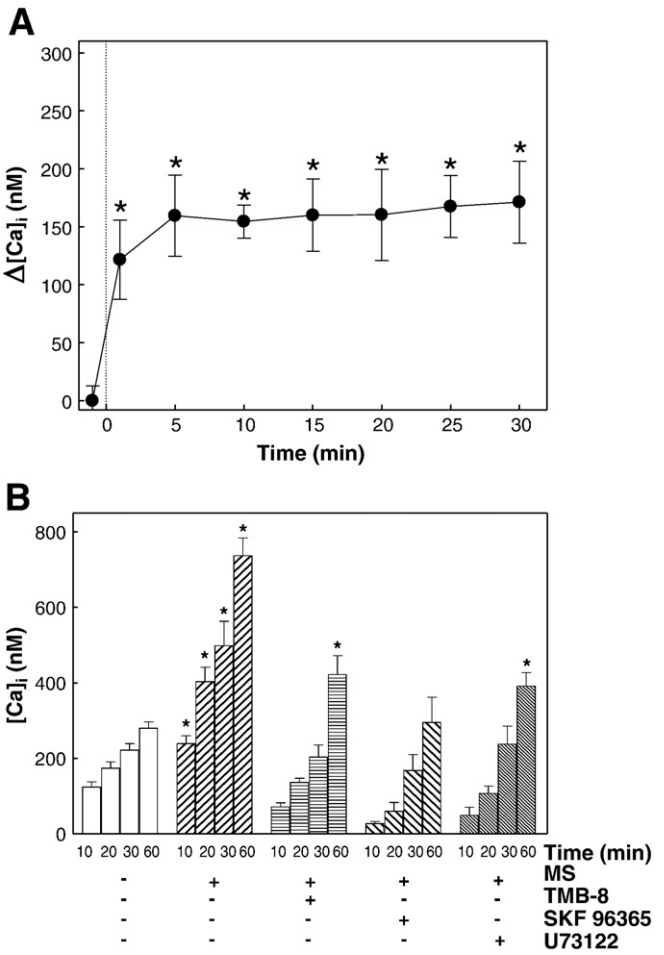

Fig. 6. MS increases the intracellular content of Ca^{2+}. Jurkat T cells loaded with the fluorescent probe FURA 2-AM were submitted to MS. (A) Intracellular Ca^{2+} concentration was measured in the samples incubated in Ca^{2+}-free medium, from the changes in the fluorescence emission of the free and Ca^{2+}-bound probe. Results are expressed as the difference between Ca^{2+} concentration measured in MS and nonstressed cells ($\Delta[Ca]_i$). Results are shown as the mean ± SEM of five independent experiments. *Significantly different ($P<0.001$) from the value obtained in nonstressed cells (two-way ANOVA test). Dotted line indicates the moment where MS was performed. (B) Effects of Ca^{2+}-mobilization inhibitors. Cells in RPMI media were preincubated for 30 min at 37 °C with TMB-8 (25 μM), SKF96365 (30 μM), or U73122 (3 μM) and submitted to MS as described above. Cellular Ca^{2+} was evaluated for 0–60 min after MS. Results are shown as the mean ± SEM of four independent experiments. *Significantly different to the value measured at the same incubation time in nonstressed cells ($P<0.001$, two-way ANOVA test).

phosphorylation of the mitogen-activated protein kinases (MAPKs) p38 and JNK increased after MS, with maximum values observed after 20–30 min after MS (Fig. 7C). The maximum NF-κB–DNA binding was observed 60 min after submitting cells to MS (Figs. 7D and E). The phosphorylation of the inhibitory peptide IκBα required for the subsequent IκBα degradation and release of active NF-κB, occurred 30 min after MS (Fig. 7D).

Given that NFAT and NF-κB nuclear translocation requires a normal microtubular dynamics [21,22], the translocation of the activated NFAT and NF-κB to the nucleus was evaluated by EMSA assays in nuclear fractions. In agreement with the kinetics of activation in total fractions, the DNA binding of NFAT, AP-1, and NF-κB in nuclear fractions reached a maximum 20, 30, and 60 min after MS, respectively (Figs. 8A and B).

To evaluate the participation of Ca^{2+} in NF-κB, AP-1, and NFAT activation upon MS, cells were incubated with the different Ca^{2+} inhibitors before MS. The effects of these inhibitors on NFAT–, AP-1–, and NF-κB–DNA binding were measured in nuclear fractions isolated 20, 30, and 60 min after MS, respectively. TMB-8 (25 μM), SKF96365

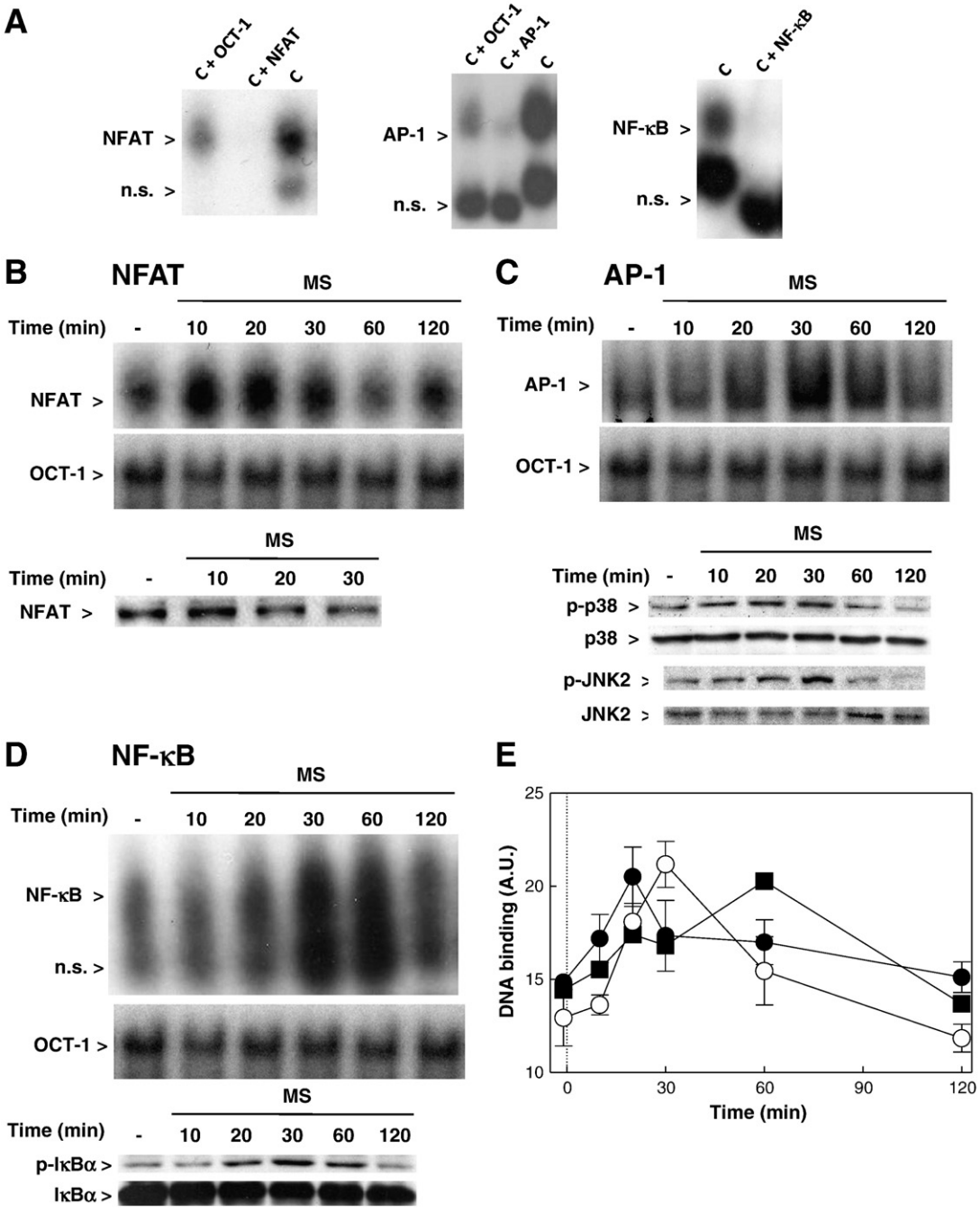

Fig. 7. MS causes NFAT, AP-1, and NF-κB activation. Jurkat T cells were submitted to MS, and total NFAT–, AP-1–, and NF-κB–DNA binding was measured in cell lysates. (A) The specificity of the NFAT–, AP-1–, and NF-κB–DNA complex was assessed by incubating a control (C) sample with a 100-fold molar excess of the nonrelated sequence OCT-1 (C + OCT-1), or of the nonradioactive NFAT (C + NFAT), AP-1 (C + AP-1), or NF-κB (C + NF-κB). (B) Kinetics of variations in NFAT–DNA binding before (−) and 10–120 min after MS. Top panel: a representative EMSA. Bottom panel: NFAT levels in total cell lysates, before and after MS, were evaluated by Western blot. (C) AP-1–DNA binding before and after MS. Top panel: a representative EMSA. Bottom panel: phosphorylated (p-p38 and p-JNK2) and total p38 and JNK2 levels in cell lysates, before and after MS, were evaluated by Western blot. (D) NF-κB–DNA binding before and after MS. Top panel: a representative EMSA. Bottom panel: phosphorylated IκBα (p-IκBα) and IκBα levels in cell lysates, before and after MS, were evaluated by Western blot. (E) After EMSA, bands were quantitated and results are shown as the mean ± SEM of four independent experiments.

(30 μM), and U73123 (3 μM) significantly inhibited MS-induced activation of NFAT, AP-1, and NF-κB (Fig. 9C). Similarly, in cells preincubated with the calcineurin inhibitor cyclosporin A (10 μM) or the PKC inhibitor Ro32-0432 (1 μM), MS-induced activation of the three transcription factors was partially prevented (Fig. 9B).

4. Discussion

T cells are continuously exposed to variations in external forces, mainly due to changes in blood pressure which is particularly high in microcirculation. In the present work, we simulated cell transit along small vessels forcing the passage of T cells through a 200-μm-diameter plastic tube which is at least, one order of magnitude higher than the average T cells' diameter (6–15 μm). MS affects membrane biophysics and cytoskeleton dynamics, leading to Ca^{2+} mobilization and the subsequent triggering of AP-1, NFAT, and NF-κB activation. Results underscore the role of the cytoplasmic membrane as a central transducer of MS into critical changes in T-cell physiology.

We first evaluated the effects of MS on cytoskeleton integrity. Both microtubules and microfilaments were affected by MS, following

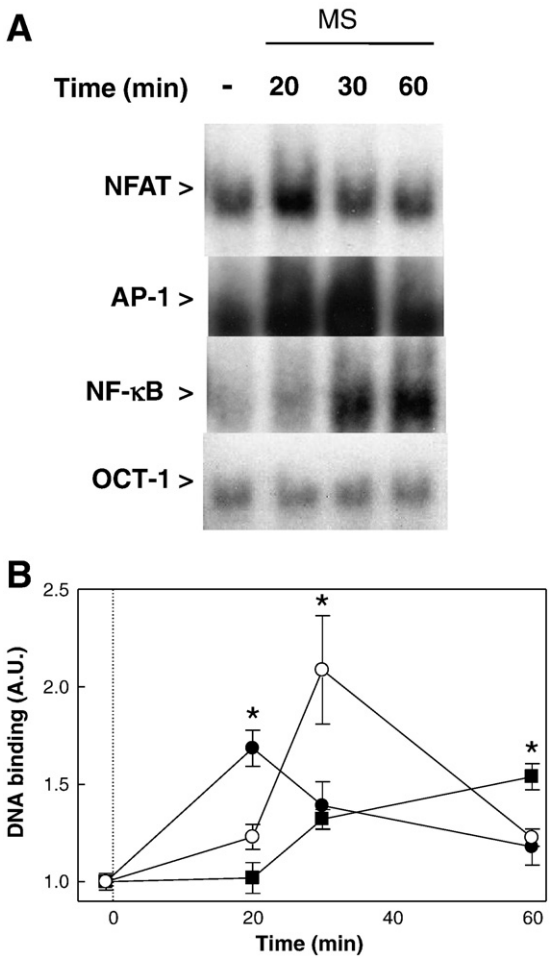

Fig. 8. MS-activated NFAT, AP-1, and NF-κB translocate to the cell nucleus. NFAT–, AP-1–, and NF-κB–DNA binding was assessed in Jurkat T cells nuclear fractions isolated from control cells (−) or after 20, 30 or 60 min after MS. (A) representative EMSA. (B) After EMSA, bands were quantitated for NFAT (●), AP-1 (○), and NF-κB (■) binding to DNA. Results are shown as the mean ± SEM of three independent experiments. *Significantly different from the value measured in nonstressed cells ($P<0.01$).

similar kinetics. This effect could be ascribed to the fact that microfilaments are in close contact with membrane lipids [23,24] and they could be rapidly affected by mechanical forces. Thus, alterations in cytoskeleton dynamics and in membrane biophysics can be closely intertwined events in MS. In fact, a rapid and significant increase in plasma membrane fluidity was found upon MS, indicating an increased disorganization of the bilayer. The alteration of membrane fluidity was restricted to the hydrophobic region of the bilayer, where lipid acid chains are located, while no changes in fluidity were observed at the superficial level of the membrane. MS-induced changes in membrane fluidity were prevented by pretreating cells with either a microfilament (jasplakinolide) or a microtubule (taxol) stabilizer. These findings support the close association of both events, alterations in cytoskeleton assembly and in membrane physical properties, as a consequence of MS.

The deformation of cytoskeleton and the lateral mobility of lipids in membranes are intertwined events [23,25]. Upon MS, pyrene excimer-to-monomer ratio decreased and did not recover the initial values within the period assessed. This could be due to MS-induced momentary disturbances in the membrane that allows the probe to reach lipid domains that were unavailable in the resting cells. These lipid domains, i.e., lipid rafts, could retain the probe even after the recovery of both cytoskeleton assembly and membrane fluidity. Lipid rafts emerge as good candidates to constitute this kind of lipid domains. When lipid rafts' organization was followed after MS, a rapid clustering of lipid rafts was observed. The initial pattern of raft distribution was achieved after 30 min after MS. Similar results were previously reported in Jurkat cells upon stimulation with phytohemagglutinin [26]. Given that lipid rafts constitute the scaffold where many signaling molecules are activated [27,28], their transient alteration can have profound consequences in cell signaling.

MS also caused plasma membrane hyperpolarization, an effect that was sustained along the period assessed. In nonexcitable cells, such as Jurkat T cells, hyperpolarization is usually a driving force for Ca^{2+} entry [29]. Even in the absence of Ca^{2+} in the incubation media, MS caused an increase in cellular Ca^{2+} concentration, and this increase was even higher when media contained 1 mM Ca^{2+}. In the latter condition, the inhibitors of PLCγ activity (U73122) or endoplasmic reticulum channels (TMB-8) partially prevented Fura-reactive Ca^{2+} increase. The inhibition of Ca^{2+} release-activated Ca^{2+} channels (CRAC) by SKF96365 also inhibited MS-induced Ca^{2+} influx. CRAC channels belong to the store-operated channels (SOCs) family and respond to a depletion of Ca^{2+} within the endoplasmic reticulum [30]. Based on our results, the increase in cytoplasmic Ca^{2+} concentration after MS can occur through the activation of PLCγ which renders IP_3 and causes the release of Ca^{2+} from the endoplasmic reticulum. In lymphocytes, PLCγ activity is closely related to lipid rafts' integrity [31] where the enzyme has to be recruited for its activation [32]. Ca^{2+} mobilization from intracellular stores could be also triggered by actin depolymerization through the opening of stretch-activated Ca^{2+} channels [33,34]. Furthermore, it has been reported that cytochalasin D, an F-actin destabilizing compound, causes a sustained increase in intracellular Ca^{2+} due to a decrease in Ca^{2+} ATPase expression [35].

Ca^{2+} is a key ion involved in many biological reactions. For example, in lymphocytes, Ca^{2+} stimulates the synthesis of pro-inflammatory cytokines [36] such as interleukin-2. This pathway is mediated by the binding of Ca^{2+} to calcineurin, a complex that stimulates phosphorylated nuclear factor of activated T cells (p-NFAT) dephosphorylation, a transcription factor that modulates the expression of several cytokines. MS resulted in a rapid activation of NFAT followed by its translocation to the nucleus. This effect was prevented by both, Ca^{2+} mobilization inhibitors and an inhibitor of calcineurin, cyclosporin A. In the current experimental model, we found that actin depolymerization and NFAT activation followed similar kinetics, results that are in agreement with previous reports showing that prolonged actin depolymerization results in a sustained NFAT activation [33,35].

Ca^{2+} also activates PKC, which in turn triggers the MAPKs cascade [1]. The activation of MAPKK results in JNK-2 and p38 phosphorylation that ultimately activate transcription factor AP-1. We found that upon MS, JNK-2 and p38 were phosphorylated, leading to AP-1 activation. Supporting a role of Ca^{2+} and PKC in AP-1 activation, MS-mediated AP-1 activation was inhibited by preincubating cells either with Ca^{2+} mobilization inhibitors or with Ro32-0432, a PKC inhibitor. Accordingly, MS due to cell stretching has been reported to activate AP-1 in different cell lines, such as bladder smooth muscle [37], mesangial cells [38], cardiac myocites [39], and vascular smooth muscle cells [40], although the biological responses vary according to the cell type. In the case of Jurkat T cells, the concomitant activation of AP-1 and NFAT could lead to the formation of a NFAT/AP-1 complex responsible for the transcription of several inflammatory genes, such as IL-2, TNFα, and cyclooxygenase 2 (Cox2) genes (for a review, see Macian et al. [41]).

Through the interaction with Carma-1 and MALT-1 present in lipids rafts, PKC can also phosphorylate IKKβ [36,42]. IKKβ activation leads to IκBα phosphorylation and degradation, releasing the active NF-κB which translocates to the nucleus and stimulates the transcription of proinflammatory cytokines (Fig. 10). Similar to that found for MS-dependent NFAT and AP-1 activation, Ca^{2+} mobilization and PKC inhibitors suppressed NF-κB activation. These results are in accordance with previous reports showing that the pharmacological

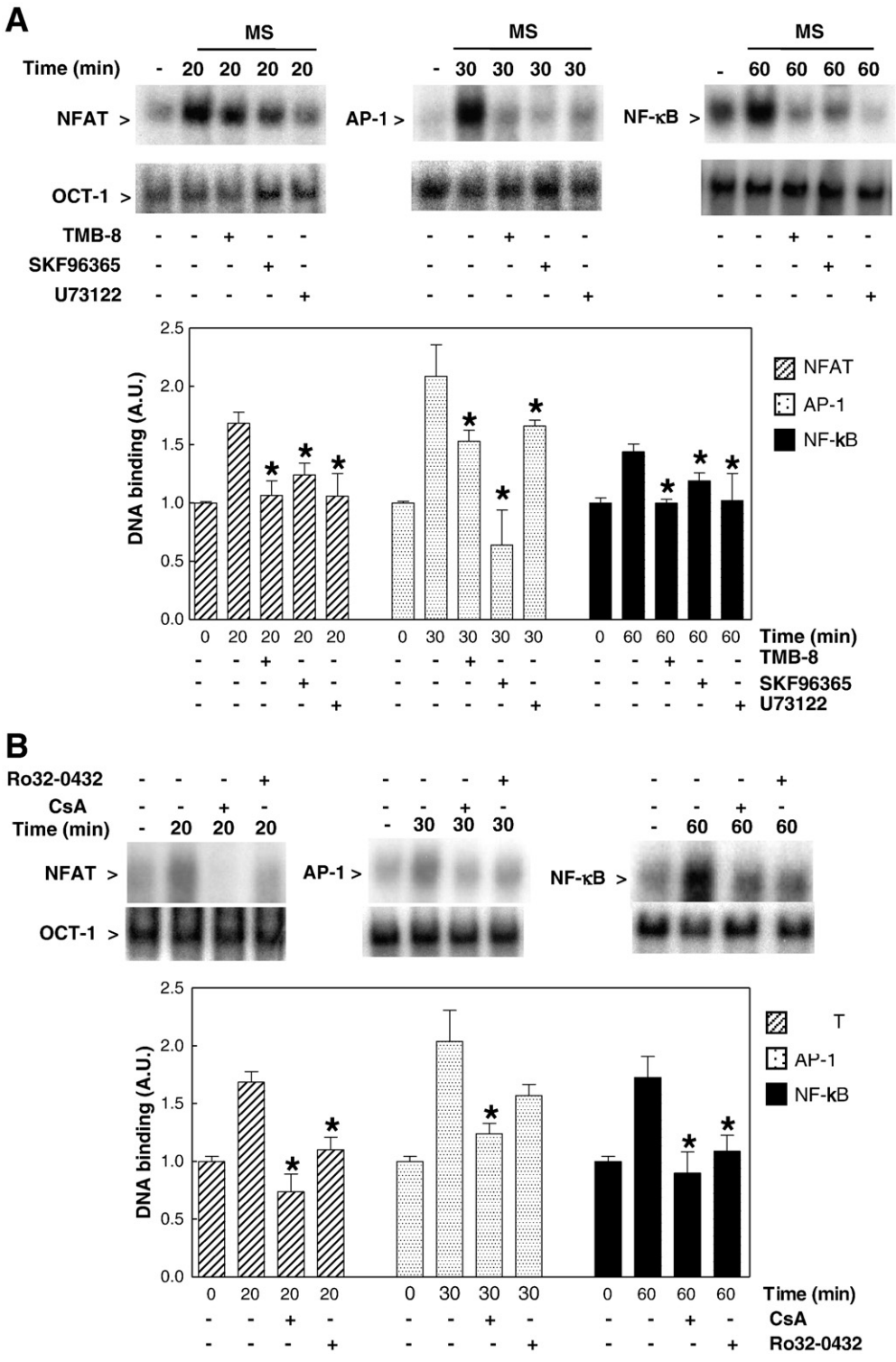

Fig. 9. Modulators of intracellular of Ca^{2+} and PKC inhibition decreases MS-mediated NFAT, AP-1, and NF-κB activation. Jurkat T cells were incubated for 1 h at 37 °C in the presence of (A) TMB-8 (25 μM), SKF96365 (30 μM), and U73122 (3 μM); (B) PKC inhibitor Ro32-0432 (1 μM) and cyclosporin A (CsA, 10 μM). After incubation, cells were submitted to MS, nuclear fractions were isolated, and NFAT–, AP-1–, and NF-κB–DNA binding was assessed by EMSA. Upper panels: representative EMSA; bottom panels: after EMSA, bands were quantitated for NFAT (▨), AP-1 (⬚), and NF-κB (■). Results are shown as mean ± SEM of four independent experiments. *Significantly different from the value measured in MS cells ($P<0.001$).

inhibition of PKC results in an inhibition of IKKβ phosphorylation, and therefore, in the prevention of NF-κB activation [43]. It has also been reported that in myelomonocytic cells, the distribution of the actin network by cytochalasin D leads to NF-κB activation [35,44]. Are et al. showed that the p65/RelA subunit of NF-κB interacts with F-actin-containing structures and that actin filaments disassembly caused RelA redistribution into actin aggregates [45].

In summary, this work demonstrates that the cell plasma membrane plays a crucial role in the multiple consequences of MS on cell physiology. The effects of MS on lymphocytes begin at the

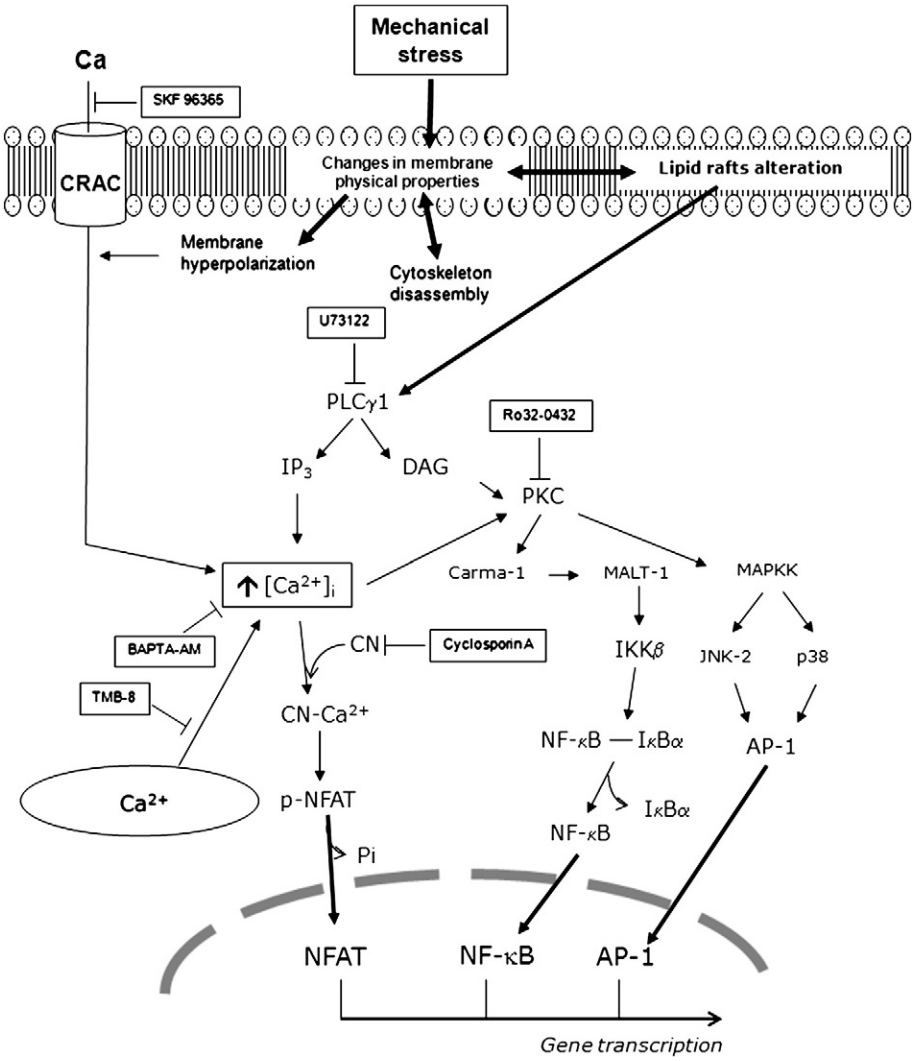

Fig. 10. Membrane-associated events are critical in the triggering of cell signals by MS.

plasma membrane level with changes in membrane rheological properties which have a tight interplay with cytoskeleton components. One consequence of those changes is the mobilization of Ca^{2+} that prompts a myriad of cell signaling pathways, including those involved in the inflammatory response. The role of recurring MS in circulating lymphocytes, as well as its consequences on the physiology of surrounding capillary endothelial cells deserves further investigations.

Acknowledgments

SVV and PIO are members of CONICET (Argentina). This work was supported by grants of the CONICET (PIP 21020), Argentina, and the University of California, Davis, USA.

References

[1] C. Li, Q. Xu, Mechanical stress-initiated signal transduction in vascular smooth muscle cells in vitro and in vivo, Cell. Signal. 19 (2007) 881–891.
[2] C.S. Chen, Mechanotransduction—a field pulling together? J. Cell Sci. 121 (2008) 3285–3292.
[3] G.M. Riha, P.H. Lin, A.B. Lumsden, Q. Yao, C. Chen, Roles of hemodynamic forces in vascular cell differentiation, Ann. Biomed. Eng. 33 (2005) 772–779.
[4] A. Gojova, A.I. Barakat, Vascular endothelial wound closure under shear stress: role of membrane fluidity and flow-sensitive ion channels, J. Appl. Physiol. 98 (2005) 2355–2362.
[5] C.V. Bouten, C.W. Oomens, F.P. Baaijens, D.L. Bader, The etiology of pressure ulcers: skin deep or muscle bound? Arch. Phys. Med. Rehabil. 84 (2003) 616–619.
[6] G. Cinamon, R. Alon, A real time in vitro assay for studying leukocyte transendothelial migration under physiological flow conditions, J. Immunol. Methods 273 (2003) 53–62.
[7] B. Anvari, J.H. Torres, B.W. McIntyre, Regulation of pseudopodia localization in lymphocytes through application of mechanical forces by optical tweezers, J. Biomed. Opt. 9 (2004) 865–872.
[8] M. Hagihara, A. Higuchi, N. Tamura, Y. Ueda, K. Hirabayashi, Y. Ikeda, S. Kato, S. Sakamoto, T. Hotta, S. Handa, S. Goto, Platelets, after exposure to a high shear stress, induce IL-10-producing, mature dendritic cells in vitro, J. Immunol. 172 (2004) 5297–5303.
[9] J. Wan, W.D. Ristenpart, H.A. Stone, Dynamics of shear-induced ATP release from red blood cells, Proc. Natl. Acad. Sci. U. S. A. 105 (2008) 16432–16437.
[10] M. Chachisvilis, Y.L. Zhang, J.A. Frangos, G protein-coupled receptors sense fluid shear stress in endothelial cells, Proc. Natl. Acad. Sci. U. S. A. 103 (2006) 15463–15468.
[11] M.P. Wymann, P. Kernen, T. Bengtsson, T. Andersson, M. Baggiolini, D.A. Deranleau, Corresponding oscillations in neutrophil shape and filamentous actin content, J. Biol. Chem. 265 (1990) 619–622.
[12] T.J. Dennerll, H.C. Joshi, V.L. Steel, R.E. Buxbaum, S.R. Heidemann, Tension and compression in the cytoskeleton of PC-12 neurites: II. Quantitative measurements, J. Cell Biol. 107 (1988) 665–674.
[13] M. Hashimoto, M.S. Hossain, T. Shimada, H. Yamasaki, Y. Fujii, O. Shido, Effects of docosahexaenoic acid on annular lipid fluidity of the rat bile canalicular plasma membrane, J. Lipid Res. 42 (2001) 1160–1168.
[14] G. Grynkiewicz, M. Poenie, R.Y. Tsien, A new generation of Ca^{2+} indicators with greatly improved fluorescence properties, J. Biol. Chem. 260 (1985) 3440–3450.
[15] J.M. Muller, R.A. Rupec, P.A. Baeuerle, Study of gene regulation by NF-kappa B and AP-1 in response to reactive oxygen intermediates, Methods 11 (1997) 301–312.
[16] M.M. Bradford, A rapid and sensitive method for the quantitation of microgram quantities of protein utilizing the principle of protein–dye binding, Anal. Biochem. 72 (1976) 248–254.

[17] F.S. Abrams, A. Chattopadhyay, E. London, Determination of the location of fluorescent probes attached to fatty acids using parallax analysis of fluorescence quenching: effect of carboxyl ionization state and environment on depth, Biochemistry 31 (1992) 5322–5327.
[18] P. Pizzo, A. Viola, Lymphocyte lipid rafts: structure and function, Curr. Opin. Immunol. 15 (2003) 255–260.
[19] M. Villalba, K. Bi, F. Rodriguez, Y. Tanaka, S. Schoenberger, A. Altman, Vav1/Rac-dependent actin cytoskeleton reorganization is required for lipid raft clustering in T cells, J. Cell Biol. 155 (2001) 331–338.
[20] A. Yamada, N. Gaja, S. Ohya, K. Muraki, H. Narita, T. Ohwada, Y. Imaizumi, Usefulness and limitation of $DiBAC_4(3)$, a voltage-sensitive fluorescent dye, for the measurement of membrane potentials regulated by recombinant large conductance Ca^{2+}-activated K^+ channels in HEK293 cells, Jpn. J. Pharmacol. 86 (2001) 342–350.
[21] G.G. Mackenzie, C.L. Keen, P.I. Oteiza, Microtubules are required for NF-kappaB nuclear translocation in neuroblastoma IMR-32 cells: modulation by zinc, J. Neurochem. 99 (2006) 402–415.
[22] G.G. Mackenzie, M.P. Zago, C.L. Keen, P.I. Oteiza, Low intracellular zinc impairs the translocation of activated NF-kappa B to the nuclei in human neuroblastoma IMR-32 cells, J. Biol. Chem. 277 (2002) 34610–34617.
[23] S. Khurana, Role of actin cytoskeleton in regulation of ion transport: examples from epithelial cells, J. Membr. Biol. 178 (2000) 73–87.
[24] G.R. Chichili, W. Rodgers, Cytoskeleton–membrane interactions in membrane raft structure, Cell. Mol. Life Sci. 66 (2009) 2319–2328.
[25] J. Li, G. Lykotrafitis, M. Dao, S. Suresh, Cytoskeletal dynamics of human erythrocyte, Proc. Natl. Acad. Sci. U. S. A. 104 (2007) 4937–4942.
[26] E. Giurisato, D.P. McIntosh, M. Tassi, A. Gamberucci, A. Benedetti, T cell receptor can be recruited to a subset of plasma membrane rafts, independently of cell signaling and attendantly to raft clustering, J. Biol. Chem. 278 (2003) 6771–6778.
[27] P. Pizzo, E. Giurisato, A. Bigsten, M. Tassi, R. Tavano, A. Shaw, A. Viola, Physiological T cell activation starts and propagates in lipid rafts, Immunol. Lett. 91 (2004) 3–9.
[28] P. Pizzo, A. Viola, Lipid rafts in lymphocyte activation, Microbes Infect. 6 (2004) 686–692.
[29] A.B. Parekh, J.W. Putney Jr., Store-operated calcium channels, Physiol. Rev. 85 (2005) 757–810.
[30] R. Penner, A. Fleig, Store-operated calcium entry: a tough nut to CRAC, Sci. STKE 2004 (2004) e38.
[31] K.F. Meiri, Lipid rafts and regulation of the cytoskeleton during T cell activation, Philos. Trans. R. Soc. Lond. B Biol. Sci. 360 (2005) 1663–1672.
[32] A. Braiman, M. Barda-Saad, C.L. Sommers, L.E. Samelson, Recruitment and activation of PLCgamma1 in T cells: a new insight into old domains, EMBO J. 25 (2006) 774–784.
[33] F.V. Rivas, J.P. O'Keefe, M.L. Alegre, T.F. Gajewski, Actin cytoskeleton regulates calcium dynamics and NFAT nuclear duration, Mol. Cell. Biol. 24 (2004) 1628–1639.
[34] S. Ito, B. Suki, H. Kume, Y. Numaguchi, M. Ishii, M. Iwaki, M. Kondo, K. Naruse, Y. Hasegawa, M. Sokabe, Actin Cytoskeleton Regulates Stretch-activated Ca^{2+} Influx in Human Pulmonary Microvascular Endothelial Cells, Am. J. Respir. Cell Mol. Biol. 43 (2010) 26–34.
[35] G. Kustermans, J. Piette, S. Legrand-Poels, Actin-targeting natural compounds as tools to study the role of actin cytoskeleton in signal transduction, Biochem. Pharmacol. 76 (2008) 1310–1322.
[36] S.L. Tan, P.J. Parker, Emerging and diverse roles of protein kinase C in immune cell signalling, Biochem. J. 376 (2003) 545–552.
[37] H.T. Nguyen, R.M. Adam, S.H. Bride, J.M. Park, C.A. Peters, M.R. Freeman, Cyclic stretch activates p38 SAPK2-, ErbB2-, and AT1-dependent signaling in bladder smooth muscle cells, Am. J. Physiol. Cell Physiol. 279 (2000) C1155–1167.
[38] Y. Akai, T. Homma, K.D. Burns, T. Yasuda, K.F. Badr, R.C. Harris, Mechanical stretch/relaxation of cultured rat mesangial cells induces protooncogenes and cyclooxygenase, Am. J. Physiol. 267 (1994) C482–490.
[39] I. Komuro, S. Kudo, T. Yamazaki, Y. Zou, I. Shiojima, Y. Yazaki, Mechanical stretch activates the stress-activated protein kinases in cardiac myocytes, FASEB J. 10 (1996) 631–636.
[40] Y. Hu, G. Bock, G. Wick, Q. Xu, Activation of PDGF receptor alpha in vascular smooth muscle cells by mechanical stress, FASEB J. 12 (1998) 1135–1142.
[41] F. Macian, C. Lopez-Rodriguez, A. Rao, Partners in transcription: NFAT and AP-1, Oncogene 20 (2001) 2476–2489.
[42] P. Narayan, B. Holt, R. Tosti, L.P. Kane, CARMA1 is required for Akt-mediated NF-kappaB activation in T cells, Mol. Cell. Biol. 26 (2006) 2327–2336.
[43] A. Sebald, I. Mattioli, M.L. Schmitz, T cell receptor-induced lipid raft recruitment of the I kappa B kinase complex is necessary and sufficient for NF-kappa B activation occurring in the cytosol, Eur J. Immunol. 35 (2005) 318–325.
[44] G. Kustermans, J. El Benna, J. Piette, S. Legrand-Poels, Perturbation of actin dynamics induces NF-kappaB activation in myelomonocytic cells through an NADPH oxidase-dependent pathway, Biochem. J. 387 (2005) 531–540.
[45] A.F. Are, V.E. Galkin, T.V. Pospelova, G.P. Pinaev, The p65/RelA subunit of NF-kappaB interacts with actin-containing structures, Exp. Cell Res. 256 (2000) 533–544.